



# Optical amplification studies in Si nanocrystals-based waveguides prepared by ion-beam synthesis

Y. Lebour<sup>a,\*</sup>, D. Navarro-Urrios<sup>b,\*</sup>, P. Pellegrino<sup>a</sup>, G. Sarrabayrouse<sup>c</sup>, L. Pavesi<sup>b</sup>, B. Garrido<sup>a</sup>

<sup>a</sup> *Departament d'Electrònica, Universitat de Barcelona, Martí i Franquès 1, 08028 Barcelona, Spain*

<sup>b</sup> *Department of Physics, Università di Trento, Via Sommarive 14, I-38050 Povo (Trento), Italy*

<sup>c</sup> *LAAS-CNRS, University of Toulouse, 7 Av. du Colonel Roche, 31077 Toulouse, France*

## ARTICLE INFO

Available online 22 August 2008

### PACS:

61.72.Tt  
78.67.-n  
42.50.Gy

### Keywords:

Light amplification  
Si nanocrystals  
Erbium  
Ion implantation  
Pump and probe  
Variable stripe length

## ABSTRACT

Light amplification has been studied in Si nanocrystals (Si-nc) based waveguides, where the active layers were obtained by ion-beam synthesis. Pump and probe measurements have been performed in both channel and rib-loaded waveguides, using short ns optical pulses from a Nd:Yag laser for pump and continuous probe signals at 650, 780 and 830 nm. The probe was quenched by carrier absorption under pumping, except at 650 nm, where a small signal enhancement was observed. On the other hand, optical amplification at 1.54  $\mu\text{m}$  has been investigated in planar waveguides based on different silicates glasses codoped with Si-nc and Er, by means of the variable stripe length technique. Positive internal gain was found only in aluminium-silicates, suggesting that this can be the best host matrix for the Si-nc:Er system in order to achieve optical amplification.

© 2008 Elsevier B.V. All rights reserved.

## 1. Introduction

During the last decades, it has been demonstrated that silicon, the leading material for microelectronics, can be used to build different kinds of photonic devices (for a review see for instance Ref. [1]). Low-loss waveguides, fast modulators, power splitters and combiners, tuneable optical filters, etc. have been already demonstrated, and thus the feasibility of silicon to manipulate light. Moreover, silicon-based detectors have been fabricated with abilities to convert a light signal into an electrical one. The scientific and technological breakthrough of the actual silicon-based photonics would consist in turning silicon into an efficient light emitter in order to combine both the functionality of silicon microelectronics with ultra-fast optical data processing and transmission on a single silicon chip.

The main potentiality of Si nanostructures (Si-nc) is their ability to provide a low-loss optically active media that can be used for achieving optical gain and then open a way to a Si-based amplifier or laser. Indeed, optical gain from Si-nc-based planar waveguides has been reported [2]. However, such very encouraging results have been proved inherent to the material preparation and treatments. On the other hand, positive signal enhancement at 1.54  $\mu\text{m}$  has been reported in active waveguides,

where Si-nc act as a sensitizer to Er ions [3]. The inclusion of Si-nc inside an Er-doped matrix induces an increase of the Er emission efficiency. This discovery has generated a lot of interest and expectations towards the realization of an optical amplifier based on such system that will work in the strategically third optical window of the optical fibre communication.

However, several limiting factors to achieve high optical gain have been reported such as carrier absorption [4], and Auger [5] for the Si-nc system, while, in addition to those phenomena, cooperative upconversion [6], excited state absorption [7], and the low Er fraction coupled to Si-nc [8] are well-known to be the main limiting factors for the Si-nc:Er system.

In this contribution, we present an optical amplification study on Si-nc embedded in SiO<sub>2</sub>-based waveguides and Si-nc:Er codoped silicates glasses-based planar waveguides, where the active layers have been obtained by ion implantation.

## 2. Si-nc active waveguides

Si-rich SiO<sub>2</sub> films were fabricated by Si multi-ion implantation into a thick thermal SiO<sub>2</sub> layer grown on a silicon substrate. Si-nc were precipitated after a thermal treatment at 1100 °C. The bottom panel in Fig. 1a represents the profiles of the Si concentrations needed to form a 0.35  $\mu\text{m}$  thick core layer with 6 at% Si excess, as calculated by the SRIM2004 simulator. Rib-loaded and channel waveguides were fabricated by

\* Corresponding authors. Tel.: +34 93 4039175; fax: +34 93 4021148.

E-mail addresses: [lebour@el.ub.es](mailto:lebour@el.ub.es) (Y. Lebour), [dnavarro@el.ub.es](mailto:dnavarro@el.ub.es) (D. Navarro-Urrios).

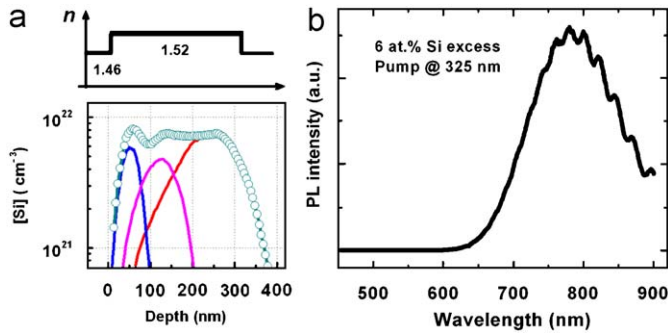


Fig. 1. (a) Si concentration and refractive index profiles of the processed waveguides, and (b) the active layer photoluminescence emission.

lithography and reactive ion etching process. The top panel in Fig. 1a represents the refractive index profile of the fabricated waveguides. A refractive index of 1.46 for the SiO<sub>2</sub> top and bottom cladding layers was considered, while a value of 1.54 was expected for the active Si-nc/SiO<sub>2</sub> layer [9]. These structures were fabricated using the same procedure as described in Ref. [10], where waveguides with an active layer of 10 at% Si excess were investigated, showing propagation losses as low as 11 dB/cm at both 633 and 780 nm wavelengths. By reducing the Si excess down to 6 at%, no degradation was found in the efficiency of the visible emission and the guiding quality of the devices. Under excitation at 325 nm from a HeCd laser, a very intense photoluminescence (PL) peaked at 780 nm was recorded from the processed layers, while defects contribution at short wavelengths was negligible, as depicted in Fig. 1b.

To investigate the PL dynamics, time-resolved (TR-PL) experiments were performed in a standard 45° configuration using 6 ns optical pulses with 10 Hz repetition rate at 355 nm of a stabilized Nd:Yag laser. The PL decays have been fitted with a stretched exponential function:  $I(t) = I_0 \exp[-(t/\tau)^\beta]$  (see for e.g. Ref. [11]), where  $\tau$  is the decay time,  $I(t)$  and  $I_0$  are the PL intensity during the decay and at  $t = 0$ , respectively. The stretched parameter  $\beta$  was found almost constant for all the data ( $\beta = 0.7$ ). Fig. 2 reveals a strong decrease of the PL lifetime as a function of the emission energy, in good agreement with previous reports in the literature [12,13]. Quantum confinement model for the Si-nc PL emission describes well this behaviour, as the oscillator strength of the interband transitions is larger for smaller Si-nc (corresponding to higher PL emission energy).

The inset in Fig. 2 presents a comparison of two PL decays obtained at the same emission wavelength by increasing the pump energy density by two orders of magnitude. The temporal decay of the PL intensity was found independent on the pump energy density, an indication of the absence of Auger-like processes in the excitons recombination [14]. This important result allows to discard the presence of Auger process, that could significantly affect the exciton recombination dynamics, and thus the stimulated emission probability.

Time-resolved pump and probe experiments were performed by focusing the spot in a stripe (approximately 100 μm wide and 1 cm long) over the channel waveguide. A continuous probe signal was fed to the waveguides butt-coupled to a tapered fibre. The guided emission was analysed by a monochromator coupled to a streak camera. A very weak probe signal was used so that the excitons population is determined only by the pump density. It is expected with the presence of the probe signal, stimulated emission process would provide the internal optical gain needed for compensating the propagation losses. Fig. 3 shows the signal enhancement, as to say, the difference between the transmitted probe intensity in presence of the pump beam (probe on, pump

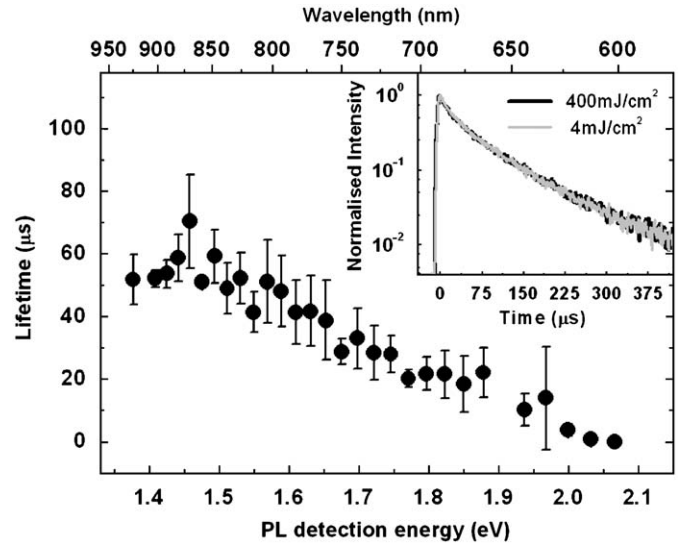


Fig. 2. Spectral dependence of the PL lifetimes. The inset reports the PL decays in normalized log scale at 780 nm for high (black) and low (grey) fluxes.

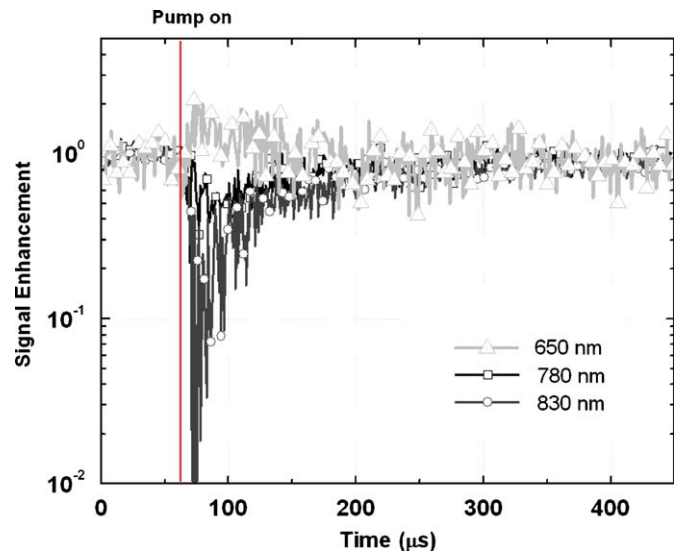


Fig. 3. Signal enhancement in log scale for different probe wavelengths. The pump energy density was fixed at 400 mJ/cm<sup>2</sup>.

on) and the guided luminescence (probe off, pump on), normalized to the probe intensity (probe on, pump off). When the probe is tuned to 780 or 830 nm, the presence of the pump severely quenches the signal. This behaviour is consistent with the presence of carrier absorption [4], i.e. part of the excitons generated by the pump successively absorb probe photons to promote electrons to higher energetic levels in the nanocrystal conduction band. It is worth to note that there is a good agreement between the carrier absorption temporal behaviour (tens of μs) and the TR-PL measurements reported in Fig. 2, because excitons population governs both dynamics. Thus, although the suppression of non-radiative decay paths (such as Auger process) provides obvious benefits in terms of PL signal, but at the same time it increases the carrier absorption probability, since the total exciton lifetime is large.

For a probe wavelength of 650 nm, the behaviour was different and a positive signal enhancement of about 2 cm<sup>-1</sup> was observed. However, it is difficult to relate this result to a stimulated

emission process, because there is almost no PL emission from the sample at this wavelength (see Fig. 1b). Moreover, the temporal behaviour of the signal rise is quite slow in comparison to the temporal characteristics of a stimulated emission in Si-nc [14].

### 3. Si-nc and Er codoped silicates glasses

Planar waveguides based on soda-lime, aluminium-silicates and silica glasses codoped with Si-nc and Er have been fabricated. The presence of the Si-nc inside the different hosts has been found to widely increase Er emission at  $1.54\ \mu\text{m}$  [15]. A Si multi-implantation scheme was adopted in order to provide a uniform Si excess background to the subsequently implanted Er atoms. Si excess ranged from 5 to 15 at%, while Er concentration was varied between  $2 \times 10^{19}$  and  $6 \times 10^{20}\ \text{cm}^{-3}$ . By isochronal annealing experiments, the best conditions that optimize the energy transfer from Si-nc to Er were investigated. A thorough structural characterization allowed to fully characterize and model the optical behaviour of the different investigated systems [15–17]. In particular, the appearance of clustering at high Er concentrations can be deleterious for the performance of the material [16]. This phenomenon has been observed by means of energy filtered transmission electron microscope (EFTEM) equipped with a gatan image filter, which adds electron energy-loss spectroscopy (EELS) analysis. By filtering the transmitted electron beam around 49 eV, it is possible to map the Er distribution. Fig. 4a represents the recorded EFTEM image revealing an agglomeration of Er ions, forming clusters of 5–10 nm in the middle of the implanted layer. Moreover, the location of the Er appears to coincide with a depletion region of Si clusters. This has been observed in the EELS profiles of Si and Er concentrations, which are represented in Fig. 4b for Si and in Fig. 4c for Er, respectively.

Optical amplification measurements in these glasses have been performed in a guided PL configuration. For this purpose the samples have been pumped with the 488 nm line of an Ar laser (resonant with an  $\text{Er}^{3+}$  transition band), focused into a  $50\ \mu\text{m}$  wide and 3 mm long stripe by means of a cylindrical lens. The emitted PL light was collected from the edge of the sample by a fibre bunch. Fig. 5 represents the results we obtained from aluminium-silicate glass, which is the only sample that showed some positive dependence with the pump power. It is worth to note that, as already reported in Ref. [17], this sample showed a cooperative upconversion coefficient one order of magnitude lower than the other two kinds of glass.

The samples were placed in such way that the pump density decreased only from the edge of the sample on, as shown by the spatial beamprofile of the pump laser (dashed line in Fig. 5a). Very weak guided PL signal was detected even with high pump power

densities because the active region where the  $\text{Er}^{3+}$  ions are placed is only 50 nm thick (see EELS spectrum in Fig. 4c). Nevertheless, we collected the guided PL signal, first as a function of the pump power, as reported in Fig. 5b, showing a slight superlinear behaviour. However, it is not possible to deduce from this result the presence of stimulated emission, since the population of the fundamental level decreases with pump power, and so does the absorption losses. Another evidence of vanishing of the fundamental level population is depicted in Fig. 5c, where an apparent narrowing of the spectrum is observed once increasing the pump power.

Finally, we performed optical gain measurements by means of the variable stripe length technique [18]. Because of the low signal problems that prevent a reliable analysis, we report in Fig. 5a (circles) only the result for the highest pump we used,  $1.7 \times 10^6\ \text{mW/cm}^2$ . Theoretical fits (solid line) based on one-dimensional model gives a net optical gain of  $0.5\ \text{cm}^{-1}$ . A sizeable experimental error ( $\pm 0.3\ \text{cm}^{-1}$ ), however, has to be taken into account. Such result indicates that at least transparency was achieved in aluminium-silicates.

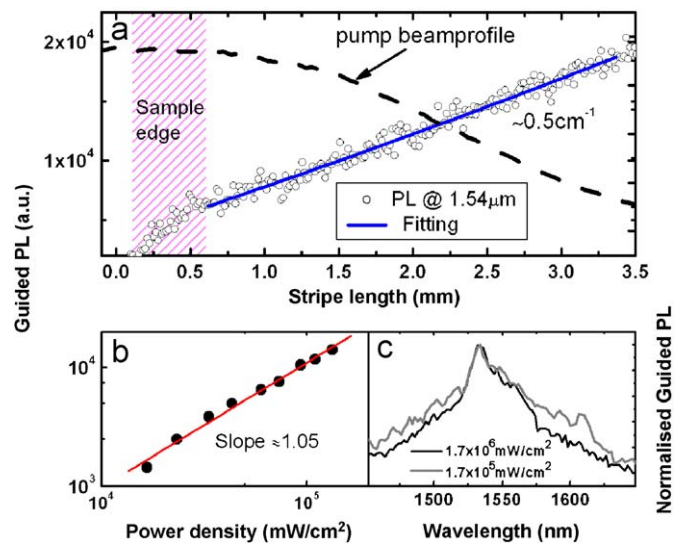


Fig. 5. Variable stripe length results in Si-nc:Er codoped aluminium-silicates glass, in (a), the pump laser beamprofile as a function of the distance to the sample edge (dashed line), and the  $1.54\ \mu\text{m}$  guided PL intensity as a function of the pumped stripe length (empty circles) together with the theoretical fit (solid line). In (b), the evolution of the  $1.54\ \mu\text{m}$  guided PL as a function of the power density. In (c), the normalized guided PL spectra for two different power densities.

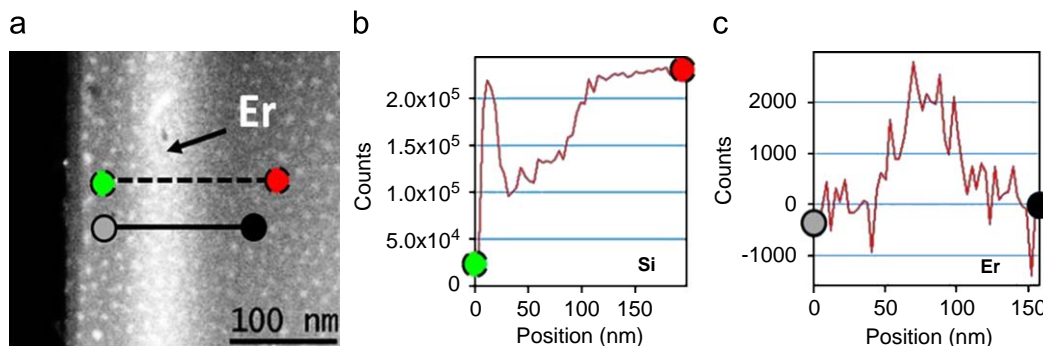


Fig. 4. (a) EFTEM image of Er distribution, (b) EELS Si Profile, and (c) EELS Er Profile.

#### 4. Conclusions

A study on light amplification has been performed in Si-nc embedded in silica-based waveguides, and Si-nc:Er codoped silicates planar waveguides. The Si-nc active region revealed a very intense visible emission, optimized by a properly tuned thermal treatment, and the absence of Auger process. Under optical pumping, however, probe signals at 780 and 830 nm were severely quenched by carrier absorption. A signal enhancement of about  $2\text{ cm}^{-1}$  was instead detected at 650 nm, whose origin is still not understood. On the other hand, for emission at  $1.54\text{ }\mu\text{m}$ , planar waveguides based on soda-lime, aluminium-silicates or silica glasses codoped with Si-nc and Er have been studied by the variable stripe length technique. Net optical gain of about  $0.5\text{ cm}^{-1}$  was obtained only in aluminium-silicate wafers, making such a matrix a suitable medium for the Si-nc:Er system to achieve light amplification.

#### Acknowledgements

This work was supported by the Spanish national Project TIC2003-07464. YL acknowledges the Spanish Ministry of Education and Science for funding his grant and his stays at LAAS and UniTN.

#### References

- [1] L. Pavesi, D. Lockwood (Eds.), *Silicon Photonics*, Topics in Applied Physics, vol. 94, Springer, Berlin, 2004; G.T. Reed, A.P. Knights, *Silicon Photonics: An Introduction*, Wiley, Chichester, West Sussex, 2004.
- [2] L. Pavesi, L. Dal Negro, C. Mazzoleni, G. Franzò, F. Priolo, *Nature* 408 (2000) 440.
- [3] J. Lee, J.H. Shin, N. Park, *J. Light. Technol.* 23 (2005) 19; N. Daldosso, et al., *Appl. Phys. Lett.* 86 (2005) 261103.
- [4] D. Navarro-Urrios, A. Pitanti, et al., *Appl. Phys. Lett.* 92 (2008) 051101.
- [5] M. Cazzanelli, D. Navarro-Urrios, F. Riboli, et al., *J. Appl. Phys.* 96 (2004) 3164.
- [6] D. Pacifici, G. Franzò, F. Priolo, F. Iacona, L. Dal Negro, *Phys. Rev. B* 67 (2003) 245301.
- [7] C.J. Oton, W.H. Loh, A.J. Kenyon, *Appl. Phys. Lett.* 89 (2006) 031116.
- [8] C. García, P. Pellegrino, Y. Lebour, B. Garrido, F. Gourbilleau, R. Rizk, *J. Luminescence* 121 (2006) 204.
- [9] J.A. Moreno, et al., *J. Appl. Phys.* 98 (2005) 013523.
- [10] P. Pellegrino, B. Garrido, C. García, et al., *J. Appl. Phys.* 97 (2005) 074312.
- [11] J. Linnros, N. Lalic, A. Galeckas, V. Grivickas, *J. Appl. Phys.* 86 (1999) 6128.
- [12] C. García, et al., *Appl. Phys. Lett.* 82 (2003) 1595.
- [13] M. Fujii, K. Imakita, K. Watanabe, S. Hayashi, *J. Appl. Phys.* 95 (2004) 272.
- [14] L. Dal Negro, et al., *Towards the first silicon laser*, in: L. Pavesi, S. Gaponenko, L. Dal Negro (Eds.), *NATO Science Series*, vol. 93, Kluwer Academic Publishers, Dordrecht, 2003, pp. 145–164.
- [15] P. Pellegrino, B. Garrido, Y. Lebour, et al., *Opt. Mater.* 27 (2005) 910.
- [16] P. Pellegrino, B. Garrido, J. Arbiol, C. García, Y. Lebour, J.R. Morante, *Appl. Phys. Lett.* 88 (2006) 121915.
- [17] Y. Lebour, P. Pellegrino, C. García, J.A. Moreno, B. Garrido, *J. Appl. Phys.* 100 (2006) 073103.
- [18] K.L. Shaklee, R.E. Nahaori, L.F. Leheny, *J. Luminescence* 7 (1973) 284.